J. Ind. Geophys. Union (April 2006)
Vol.10, No.2, pp.101-117

Heat storage variability in the Indian Ocean using Topex/ Poseidon Altimeter Data

B.H.Vaid, C.Gnanaseelan*, B.Thompson, Ayantika De and P.S.Salvekar
Indian Institute of Tropical Meteorology, Dr.Homi Bhabha Road, Pashan, Pune – 411 008
*E-mail: seelan@tropmet.res.in, pss@tropmet.res.in

ABSTRACT
Sea surface height anomalies (SSHA) derived from the Topex/Poseidon (T/P) satellite are used for computing heat storage anomalies (HSA) and heat storage rates (HSR) over the north Indian Ocean [20°S – 25°N and 35°E – 115°E] for a period of 10 years (1993-2002). In normal years during September to November positive HSA and HSR were observed in the region 10°S - Equator, 90°E - 110°E. But during the years 1994 and 1997 negative HSA and HSR were observed in this region, this interannual variability has recently been addressed as Indian Ocean Dipole (IOD). The heat content anomaly clearly showed the existence of the dipole like structure in the equatorial Indian Ocean (IO) in 1994 and 1997. The T/P measurement showed large SSHA in the western equatorial Indian Ocean during 1994-1995 and 1997 -1998 IOD events that represent the oceanic response to the surface wind forcing. These anomalies in turn played an important role in forming the sea surface temperature anomalies (SSTA). The 1997 Dipole mode structure was observed to be stronger than 1994 and that can be clearly seen in calculated HSA, HSR, T/P SSH anomalies, thermocline depth (D20) anomaly derived from Simple Ocean Data Assimilation (SODA) and in HADISST anomaly. The Rossby wave propagation is found to have a good correlation with the heat content anomaly derived from Topex/Poseidon sea surface height anomalies. During the dipole years 1994-95 and 1997-98 the anomalous westward propagation of SSHA and HSA were clearly observed especially in the region south of 7°S and strengthened in 80 - 90°E belt. Wind stress curl anomalies play an important role in strengthening this propagation in 80-90°E and hence warming the west Indian Ocean in the early months of 1998. It was seen that positive and negative dipole years are inversely correlated in the southeastern equatorial Indian Ocean (10°S - Equator, 90°E -110°E). To understand the interannual variability of upper ocean SSHA, Complex Empirical Orthogonal Function (CEOF) has been applied to T/P SSHA and HSA. IOD has been shown to be the leading mode of the interannual variability of the upper ocean SSHA and HSA. The westward propagation of the phase is in agreement with the sea saw thermocline variability observed in the equatorial Indian Ocean.

INTRODUCTION

The knowledge of sea surface height (SSH) or SSHA is very essential for climate and oceanographic studies as it indirectly represent the thermocline structure (or its anomaly) and the heat source available for the air sea interface processes. The SSHA are caused by dynamical and thermodynamical processes in the ocean on various temporal and spatial scales. Changes in oceanic heat storage (HS) are associated with density changes in the water column and thus, with the SSHA (Gill & Niiler 1973). Estimates of HS are traditionally based on in-situ measurements (Wyrtki & Uhrich 1982; Yan et al., 1995) or on climatological datasets (Hsiung, Newell & Houghtby 1989; Moisan & Niiler 1997). White &Tai, (1995) derived a linear relationship between the SSHA measured by T/P and the HS estimated from Expendable Bathy Thermograph (XBT) data and found correlations greater than 0.6 over the northern hemisphere. Chambers, Tapley & Stewart (1998) found good agreement between T/P based HSA estimates and those from the Tropical Ocean-Atmosphere (TAO) buoys. Regardless of source, the heat that enters a water column decreases its density and increases its height, causing a local anomaly. Therefore, the sea surface height variations reflect, to a large extent, the amount of heat locally stored. As HSA has direct relation with T/P SSHA, in this study we explore the interannual variability in the HSA from the T/P SSHA

signals. Two features are common to T/P SSHA [or h(x,t)], at most latitudes: the basin-scale non-propagating variability and the meso-scale to large-scale westward propagating signal.

The basin-scale signal is mostly due to seasonality and advection. The westward propagating signal has a temporal scale from months to years and spatial scale that decreases from the equator to the poles. These scales indicate that the westward propagating signals observed in the equatorial region are long baroclinic Rossby waves. These Rossby waves are not necessarily free and can be influenced by wind forcing, topography and other effects (Killworth & Blundell 1999, Samelson & Blundell 1992). Infact the Rossby waves are the large scale dynamical response of the ocean to wind forcing and buoyancy forcing (heating and cooling) at the eastern boundaries and the ocean interior. They can also be generated by perturbations along the eastern boundaries associated with coastally trapped waves originating at low latitudes (White 1985). Their surface manifestation might appear as slight rising of the mean SSH by a few centimeters and an increase in SST by a fraction of a degree. Possible stimuli include strong changes in wind forcing, variations in current and the passage of poleward-propagating Kelvin waves. The resultant baroclinic Rossby waves have a velocity structure in the meridional direction, and change the height of the thermocline by tens of meters. Their effect on reaching the west is to intensify the western boundary current, and possibly to alter its position and thus change the ocean's modification of the atmosphere (Jacobs et al., 1994).

To understand better the complex ocean-atmosphere coupled system [eg., Indian Ocean dipole (IOD)], and especially the likelihood of significant climate change, one needs a good understanding of Rossby waves — where they occur, their amplitude, and particularly their speed of propagation, which determines the timescale for ocean-atmosphere feedback. Rossby waves propagate zonally, along the equator, but also along other latitudes. IOD events (Saji et al., 1999; Webster et al., 1999) are believed to be a key factor to understand the mechanisms responsible for climate change in the tropical IO. IOD event starts with anomalous SST cooling along the Sumatra- Java coast in the eastern IO during May-June. The normal equatorial westerly winds during June-August weaken and reverse direction. And an IOD event peaks in September - October, with warmer than usual SST over large parts of the western basin (Saji et al., 1999). Several studies were carried out to explain the mechanism for formation of IOD (Behera, Krishnan & Yamagata 1999, Murtugudde, McCreary & Busalachhi 2000, Vinayachandran, Saji & Yamagata 1999, Gnanaseelan et al., 2003) and its effect on Indian summer monsoon rainfall (Ashok, Guan & Yamagata 2001). There are differences in opinion about the mechanism responsible for the interannual variability such as IOD. One school advocates the major role of surface heat fluxes (Li et al., 2003) in the evolution of interannual SSTA and other one promotes the dynamical importance of winds (Murtugudde & Busalacchi, 1999, Murtugudde, McCreary & Busalachhi 2000) in addition to the surface heat flux. Recent investigations using a variety of ocean models suggest that the SST modulation is largely due to oceanic processes, mainly vertical and horizontal advection and upwelling (Behera, Krishnan & Yamagata 1999; Murtugudde, McCreary & Busalachhi 2000). In turn the oceanic processes are the result of the ocean adjusting through equatorial wave dynamics to the strong equatorial wind anomalies associated with triggering of IOD events (Rao et al., 2002; Feng & Meyers 2003). In contrast, Annamalai et al., (2003), Lau & Nath (2003) have raised the possibility of an external trigger for the initiation of IOD. Prasad & McClean, (2004) found that internal oceanic processes within the Arabian Sea are primarily responsible for western equatorial Indian Ocean warming.

The involvement of ocean dynamics suggests a certain amount of predictability to the IOD development once it is triggered. Currently however it is not clear what triggers IOD events, though there are various hypotheses suggesting different mechanisms. For instance, due to strong correlation between IOD and ENSO events during boreal fall, Xie et al., (2002) suggested that ENSO is a possible trigger for IOD events. However a number of strong IOD events have occurred during the non ENSO years (Saji & Yamagata 2003). Recent studies suggest that some of the independent IOD events may be forced by either intraseasonal oscillations (Li et al., 2003) or monsoon variability (Wang, Wu & Li 2003). On the other hand, the possibility of IOD as a self-sustained oscillation has also been suggested (Yamagata et al., 2002). Further a strong impact of IOD events on local climate variability is hinted in recent studies. Significant signals of IOD on rainfall over equatorial East Africa (Clark, Webster & Cole 2003), Indian subcontinent (Ashok, Guan & Yamagata 2001) and Sri Lanka (Lareef, Rao & Yamagata 2003) have been recently reported.

As far as dynamics and thermodynamics related to IOD is concerned, it has been understood that the enhanced atmospheric convection (ascending motion) over the monsoon region of India and east Asia, the warm central IO region and strong vertical subsidence

over the cold south east tropical Indian Ocean (SETIO) region maintained the anomalous surface wind forcing that was responsible for the SETIO cooling during dipole years (Behera et. al 1999). The SETIO region in turn acted as an important source of moisture so as to sustain the anomalous convection. These findings clearly demonstrate the existence of a feed back mechanism between atmospheric convection and SST in the tropical IO. The changes in the SST during the IOD events are found to be associated with the changes in the surface wind over the central equatorial IO. In fact, winds reverse direction from westerlies to easterlies during the peak phase of the positive IOD events when SST is cool in the east and warm in the west. The effect of the wind is even more significant at the thermocline depths through the oceanic adjustment process (Rao et al., 2002). These changes in surface winds and oceanic conditions are coupled with the changes in the atmospheric convection through either convergence or divergence of the moist air.

Using a simple Matsuno-Gill type model, Saji and Yamagata (2002) have also shown that the atmospheric linear response to such changes in the heat source of the eastern IO strengthens the easterly wind anomalies, which in turn are responsible for the evolution of the SST dipole. Ashok, Guan & Yamagata (2001) have further confirmed this using a more sophisticated general circulation model. It has been understood that large scale winds over the IO have two anomaly patterns that affect the dynamics of the equatorial IO in a significant manner, first is the easterly anomaly which is related to the weakening of the Walker circulation and second is the strong upwelling favorable along shore anomaly which is more or less related to the strengthening of the Hadley circulation over the eastern part of IO (Vinayachandran, Saji & Yamagata 1999). More over Vinayachandran et al., (2002) reported that during the positive phase of the dipole mode, easterly wind anomalies excite upwelling equatorial Kelvin waves. This Kelvin wave, on reaching the eastern boundary, lifts the thermocline in the eastern equatorial IO and reflects as westward propagating Rossby waves. As the wind anomalies relax, the upwelling is replaced by downwelling which leads to the decay of SST anomalies. The collapse of the upwelling gives rise to a downwelling Rossby wave during the years following positive IOD (1995 and 1998). In the tropics, the oscillations of the thermocline are generally reflected in SSH variations. Therefore positive SSH anomalies correspond to a deeper thermocline in the SW IO during peak dipole time. Thus the large cooling in the eastern IO during positive IOD is mainly due to upwelling of cold water that take place off the coast of Sumatra. The oceanic Rossby waves are essential in linking the anomalous wind and SST off Sumatra and subsurface temperature variations in western IO.

DATA AND METHODOLOGY

The heat content anomalies are derived from monthly T/P sea level anomalies (η) by using the relation.

$$\Delta H = \rho Cp \Delta(\eta)/ \alpha \quad (1)$$

where Cp is the specific heat at constant pressure, a is the thermal expansion coefficient values and are same as Chambers & Tapley (1997). Thus we can relate thermal sea level changes from mean sea level to heat storage anomalies via the coefficient α, ρ and Cp.

The heat storage rates are calculated by the relation

$$\Delta H /\Delta t = \rho Cp \Delta(\eta)/ \alpha \Delta t \quad (2)$$

The individual contributions of all the wave components of different periods and characteristics are separated from 10 days SSHA (h_o) [data from 1993 – 2002] signal using a two dimensional Finite Impulse Response (FIR) filter. FIR filters are based on convolution of two sequences, the original data h_o, and the filter f, resulting in the filtered data h_f. It not only filters Rossby wave components but also meso-scale eddies, meandering currents, instability waves, and Kelvin waves all of which contribute to the SSH variability. Including these processes, h_o is

$$\eta_o = \eta_t + \eta_{24} + \eta_{12} + \eta_6 + \eta_3 + \eta_1 + \eta_K + \eta_E + \eta_r \quad (3)$$

where η_t is the non-propagating basin-scale thermosteric signal. η_{24} to η_1 are the westward propagating Rossby waves with approximate periods of 24, 12, 6, 3, and 1.5 months. η_K is present only in the equatorial region as a fast eastward propagating signal identified as equatorial Kelvin waves. η_E is the meso-scale eddy field that, outside the tropical region, has amplitude comparable to that of Rossby waves. η_r is the residual dominated by small scale or high frequency signals and instrument noise. In the present case $\eta_o(x,t)$ is a function of longitude and time; therefore the filter f(i,j) is function of longitudinal lag i and temporal lag j. The filtered matrix η_f (x,t) is obtained from

$$\eta_f(x,t) = \sum_{i=-m}^{m} \sum_{j=-n}^{n} \eta_o(x+i, t+j) f(i,j) \quad (4)$$

The size of filter is controlled by parameters m and n. The filter is applied to separate the Rossby and Kelvin waves of different periodicity. Different functions were used to filter different components

given in equation (3). However annual Rossby waves only are discussed in this paper. For more detail about the FIR filter please refer (Polito, Sato & Liu 2000). Surface winds derived from National Center for Environmental Prediction (NCEP) and National Center for Atmospheric Research (NCAR) reanalysis data product (1993-2002) were also taken in this study. D20 anomalies and HADISST from period 1993-2002 were also used in this study.

RESULTS AND DISCUSSION

IOD structure in HSA, HSR, HADISST anomalies and in D20 anomalies

When ocean is heated from the surface the water expands, so the SSH rise and this infact have direct relation with the thermocline variability (Chambers, Tapley & Stewart 1998). As heat storage has direct relation with SSHA (Chambers & Tapley 1997) and Rossby waves are found to be the main mechanism of energy transfer among the ocean basin (Gill 1982), we compared calculated HSA and HSR with Rossby wave components obtained from SSHA. Heat storage and heat transport in the IO are two important processes and have immediate implications in the overlying airmass. As discussed in the introduction, the SSH rise has a strong positive correlation with the ocean warming. Surface warming implies that a

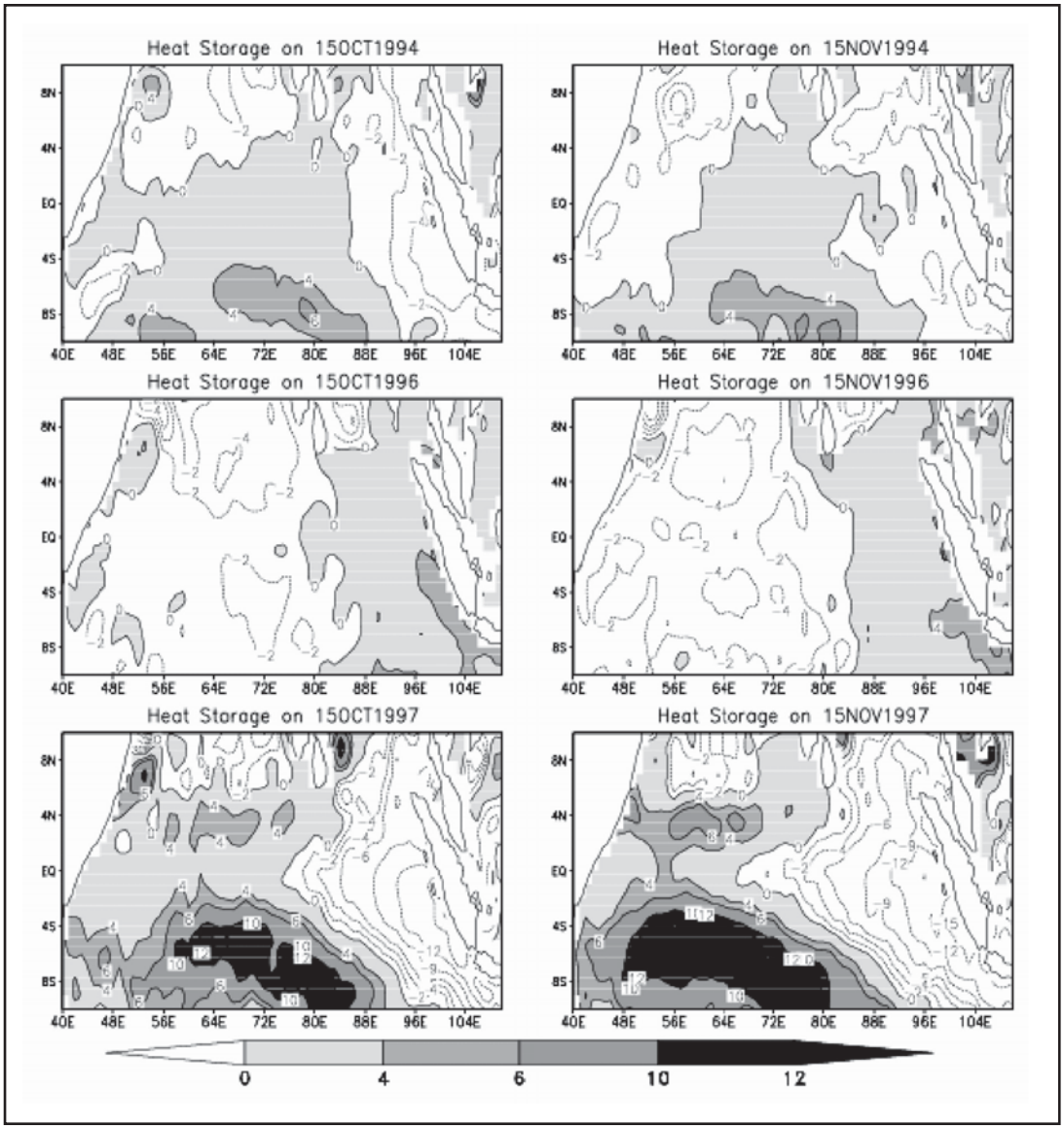

Figure 1. Heat storage anomalies (10^8 J/m^2) for 1994, 1996 and 1997.

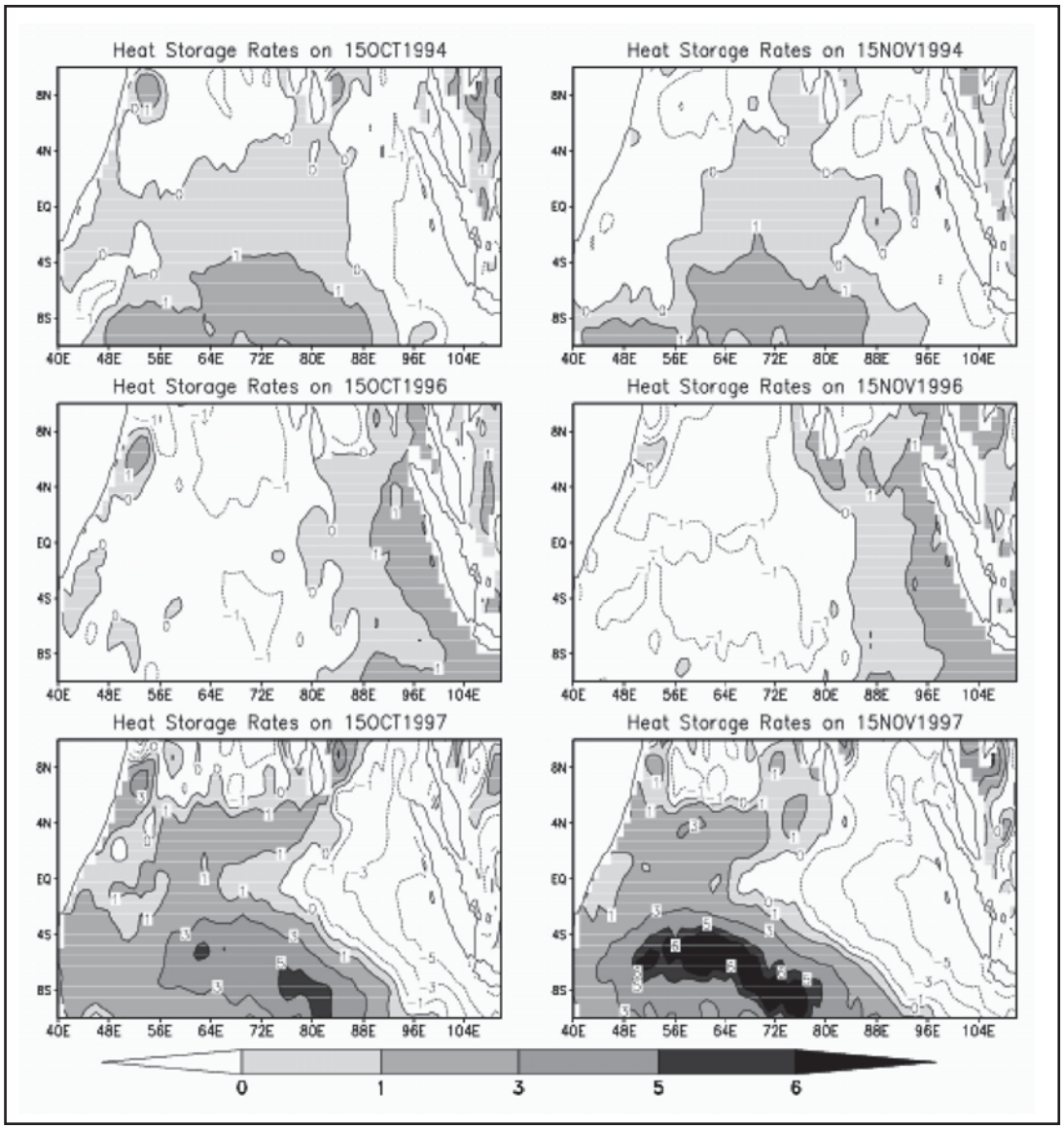

Figure 2. Heat storage Rates (10^2 W/m^2) for 1994, 1996 and 1997.

connection between the internal oceanic heat storage and atmospheric warming is possible via surface heat fluxes. In other words, this connection shows that in this region the ocean-atmosphere coupling through thermodynamics is possible. The anomalous heat storage observed from T/P is of the order of 10^9 J/m^2, a significant fraction for the equatorial IO where the total heat content of the upper 50m or so is in the order of 10^{10} J/m^2. Figure 1 shows HSA (in 10^8 J/m^2) for 1994, 1996 and 1997. In October and November 1996 the positive HSA was of the order of 2 x 10^8 J/m^2 and 4 x 10^8 J/m^2 respectively in the region 10^{o}S - Equator, 90-110^{o}E (hereafter eastern IOD box) and low HSA in the region 10^o S - 10^{o}N, 50-70^{o}E (hereafter western IOD box). Contrasting features were evident in October and November 1994 and 1997. It is clear from Fig. 1 that low HSA has been seen in eastern IOD box and high in the western IOD box. This unusual event in October 1994 and 1997 is identified as IOD. Further in 1994 peak cooling is seen in October (of the order of -4 x 10^8 J/m^2) and this cooling extend has been found to cover the longitudinal distance from 110^{o}E to 85^o E of equatorial IO. But in 1997 peak value of cooling is found in November 1997 (of the order of -15X 10^8 J/m^2) and extended from 110^{o}E to 68^{o}E. As far as western IOD box is concerned, very high value of HSA were seen in October – November 1997 and October 1994. But 1997 values were higher than 1994, which support the fact that 1997 event is stronger than 1994. Infact it

has been noticed from previous studies that the 1997 IOD event is intense and was associated with severe floods in eastern Africa and droughts over Indonesia. It was the strongest dipole recorded in history and was accompanied by massive fires in western Indonesia and the widespread death of coral reefs in the IO. Developing a better understanding of the natural dynamics and effects of the IOD is essential for improved long-range forecasts of droughts and floods in these regions.

In Fig. 2, the HSR are presented for the years 1994 and 1996, 1997 and in October 1994 and 1997 low HSR were observed in the eastern IOD box and high HSR values were observed in the western IOD box. Also in October - November 1996 (Fig. 2) high HSR are found between eastern IOD box and low heat storage rates are found in the western IOD box. Infact from left and right panels of Fig. 2 it is evident that 1997 dipole event was stronger than 1994 one.

Index to quantify the IOD has been defined (Saji et al., 1999) as the SST anomaly difference between the western IOD box and eastern IOD box. When the IOD index is positive (west is warmer than east), it leads to droughts (locally known as Tuarang) over the

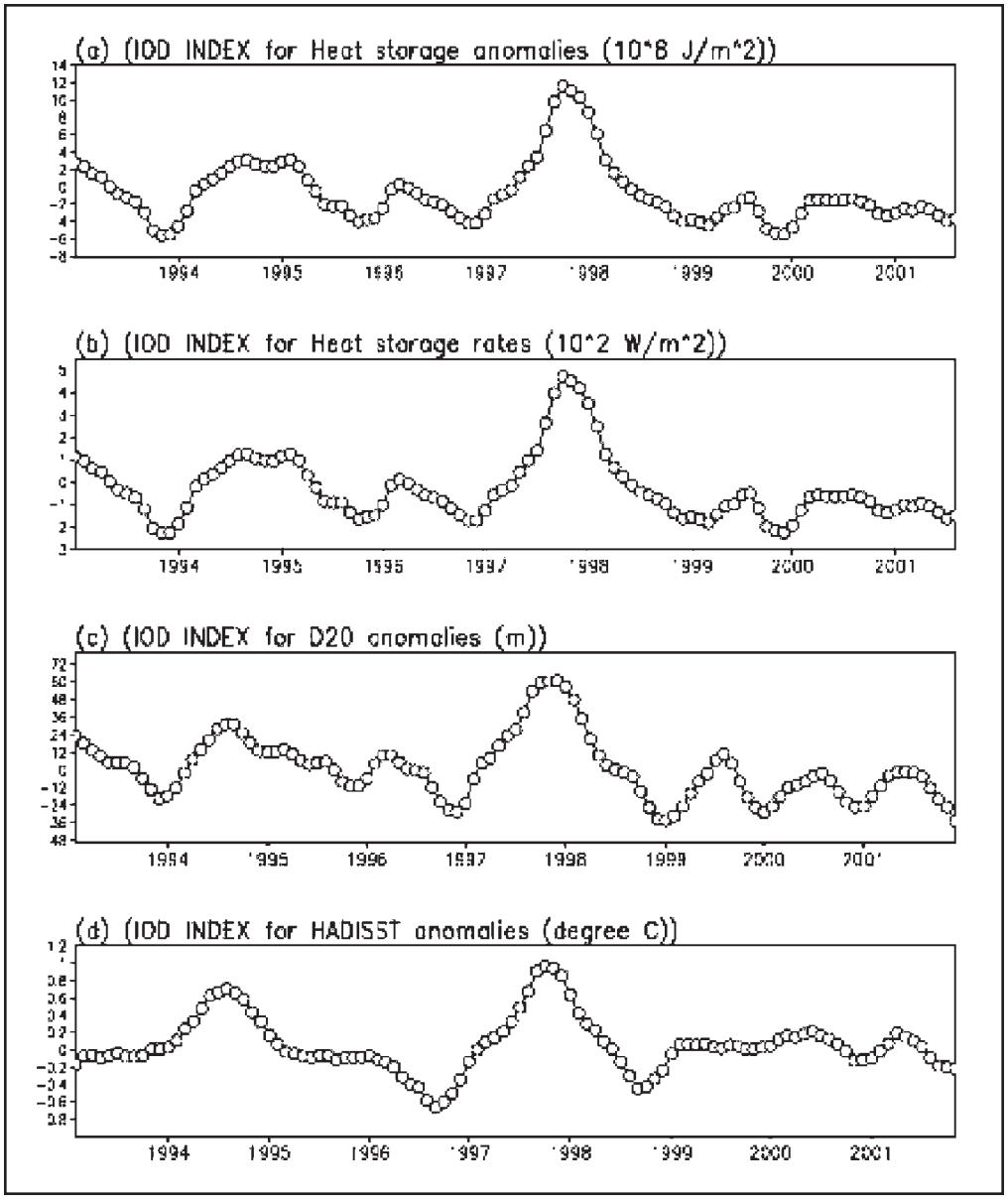

Figure 3. (a) IOD Index for Heat storage anomalies (10^8 J/m^2), (b) IOD Index for Heat storage rates (10^2 W/m^2), (c) IOD Index for D20 anomalies (m), (d) IOD Index for HADISST anomaly (degree C).

Table-1

Region 1	
Heat Storage Anomalies	D20 Anomalies
Oct. 94, Ac =.47751	Oct. 94, Ac =.64236
Oct. 96, Ac =.45502	Oct. 96, Ac =.61128
Nov. 97, Ac =.31152	Nov. 97, Ac =.47195

Region 2		
Heat Storage Anomalies	Biennial Rossby waves	D20 Anomalies
Oct. 94, Ac =.51993	Oct. 94, Ac =.71756	Oct. 94, Ac =.55834
Oct. 96, Ac =.29735	Oct. 96, Ac =.57692	Oct. 96, Ac =.54149
Nov. 97, Ac =.58274	Nov. 97, Ac =.89233	Nov. 97, Ac =.60053

Indonesian region and heavy rains and floods over the east Africa. When the sign reverses, these anomalous fluctuations also swing to the opposite phase. Fig.3 shows (a) IOD Index for Heat storage anomalies (10^8 J/m^2) (b) IOD Index for Heat storage rates (10^2 W/m^2) (c) IOD Index for D20 anomalies (m) (d) IOD Index for HADISST anomaly (degree C). It can be illustrated that calculated IOD index for (a), (b), (c) and (d) are well comparable with the IOD index calculated by Saji et al., (1999).

Anomalous Rossby wave propagation during 1994-1995 and 1997-1998

Fig.4 shows the T/P SSHA (cms), HADISST anomaly (degree C) and D20 during October /November 1994, 1996 and 1997. It was observed that dipole like structure was clearly seen in T/P SSHA, HADISST anomaly and D20 anomalies and are comparable with the dipole structure found in HSA (Fig. 1) and HSR (Fig. 2). Further Fig. 4 clearly shows evidence of upwelling Rossby waves in T/P SSHA and D20 anomalies [which is same as the upwelling Biennial Rossby waves (Gnanaseelan et al., 2005)] during 1994 and 1997. Evidence of upwelling biennial Rossby waves from the eastern equatorial IO during 1994 and 1997 has been reported by Gnanaseelan et al., (2005). From Fig. 4 it can be said that in October 1994 the upwelling Rossby waves are found extended from 110°E to 85°E. While in November 1997 these extended upto 68°E. Also in Fig. 1 and Fig. 2 and 4 it was seen in 1994 that the peak cooling in October covered the longitudinal distance from 110°E to 85°E of IO. In 1997 peak value of cooling in November extend from 110°E to 68°E. Infact signal which can be seen in T/P SSHA was result of biennial propagation of Rossby wave which has been extensively studied by Gnanaseelan et al., (2005). In order to study the pattern of T/P SSHA over eastern IOD box, area average of T/P SSHA was done over the same region (Fig.5).

The warming in the western IO has been attributed to i) westward propagating Ekman ridge around 10°S that suppress local upwelling in the west (Webster et al., 1999), ii) weak summer monsoon winds and the enhanced precipitation forcing which resulted in barrier layer structure (Murtugudde, McCreary & Busalachhi 2000), iii) weak winds and reduced evaporation in the west, together with increased precipitation and thermocline deepening due to reduced eastward transport resulting from the trade wind shift (Saji et al., 1999), iv) warming outside of the equatorial waveguide was due to the changes of latent heat flux indused by wind speed and the effect was most significant during the summer / fall of 1997 (Yu & Rienecker 2000), v) the biennial Rossby wave signal of 2 – 3 cms magnitude [Gnanaseelan et al., 2005]. However, still it needs more discussion/debate in the subject. We have also looked into the persistence of western warming to early 1995 and 1998 with more warming in 1998 than 1995. The substaining of the western warming in 1998 has been attributed to downwelling Rossby waves by Murtugudde, McCreary & Busalachhi (2000). Figs 6 and 7 show the time longitude plots of T/P SSHA and HSA at (a) average of 5.5°S to 2.5°S (b) average of 10.5°S to 5.5°S (c) average of 12.5°S to 7.5°S. Time longitude plots of T/P SSHA are almost found to be coinciding with time longitude plots of HSA. Infact it stresses the role of thermal expansion coefficient played in HSA over this part of the region. The strong cooling observed in the eastern IO in October and November 1997 is due to the propagation of upwelling Rossby waves as discussed above. Central and right panels of

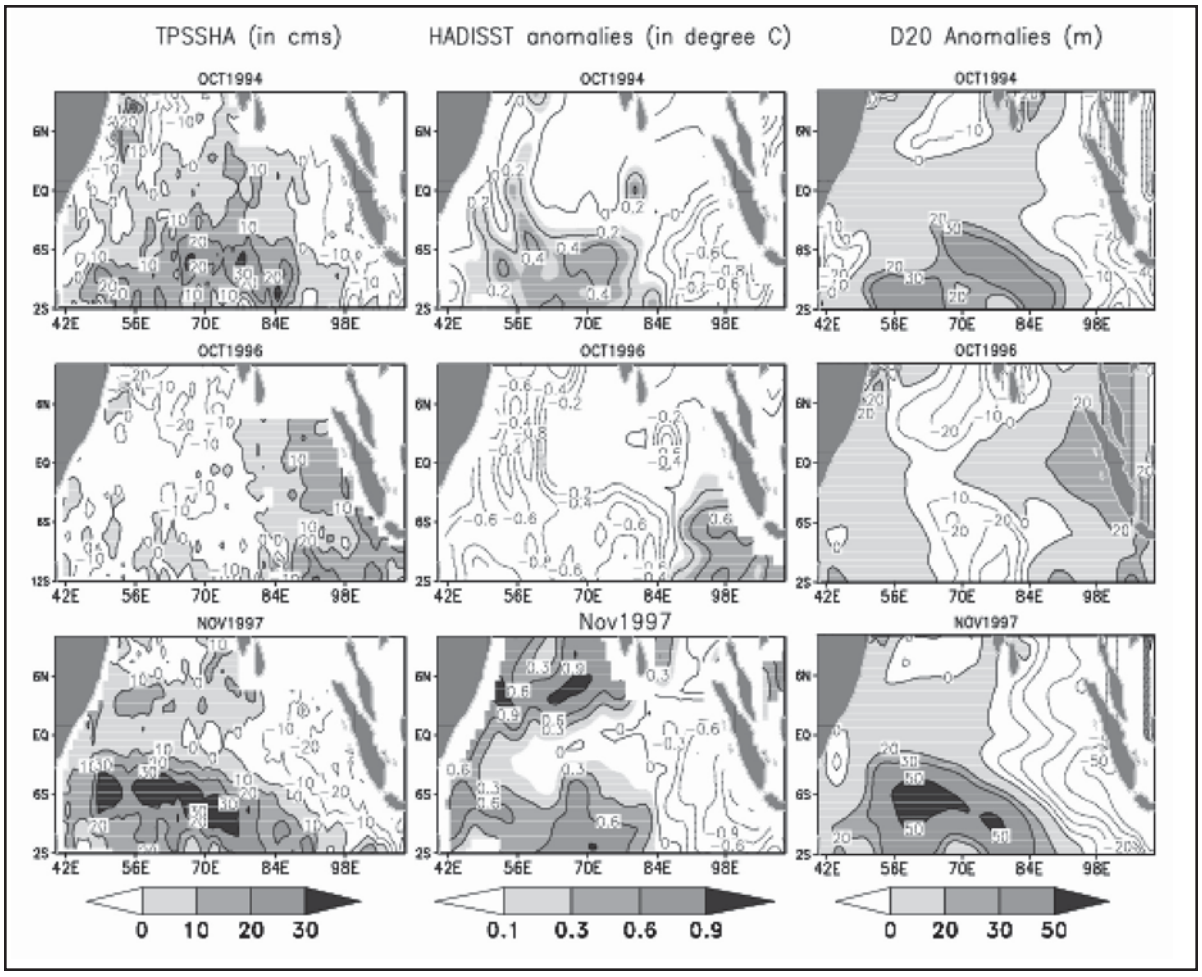

Figure 4. T/P SSHA (cms), HADISST anomaly (degree C) and D20 anomalies (m) for 1994, 1996 and 1997.

Fig. 6 and 7, show the propagation of upwelling Rossby waves from October –November 1997 which is responsible for the central IO cooling which has been found in October 1998 – March 1999.

Further evidence of central cooling has also been seen in October 1995 – March 1996 but were weaker than October 1998 – March 1999. This may be due to the difference in the strength of upwelling Rossby waves caused due to the anomalous southeasterly winds (Vinayachandran et al., 2002). These anomalies appear few months earlier during 1994. The easterly wind anomalies along the equator persist through early 1998, whereas they decay considerably during early 1995 (Vinayachandran et

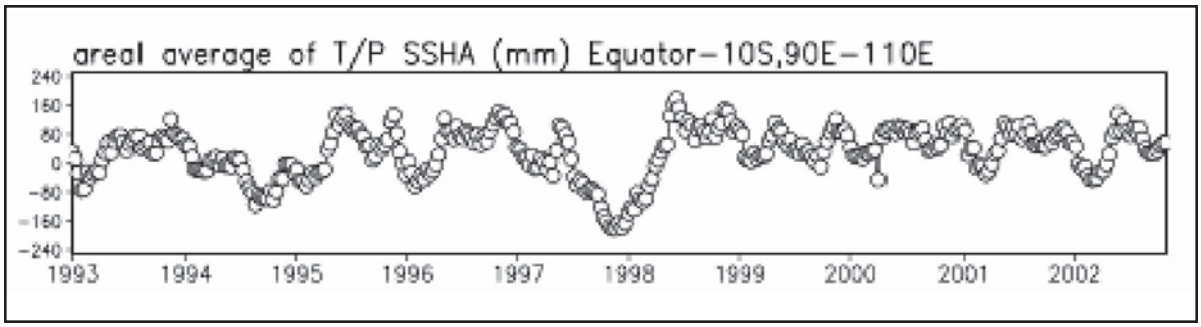

Figure 5. Area average of T/P SSHA (mm) over 10°S - Equator, 90°-110°E.

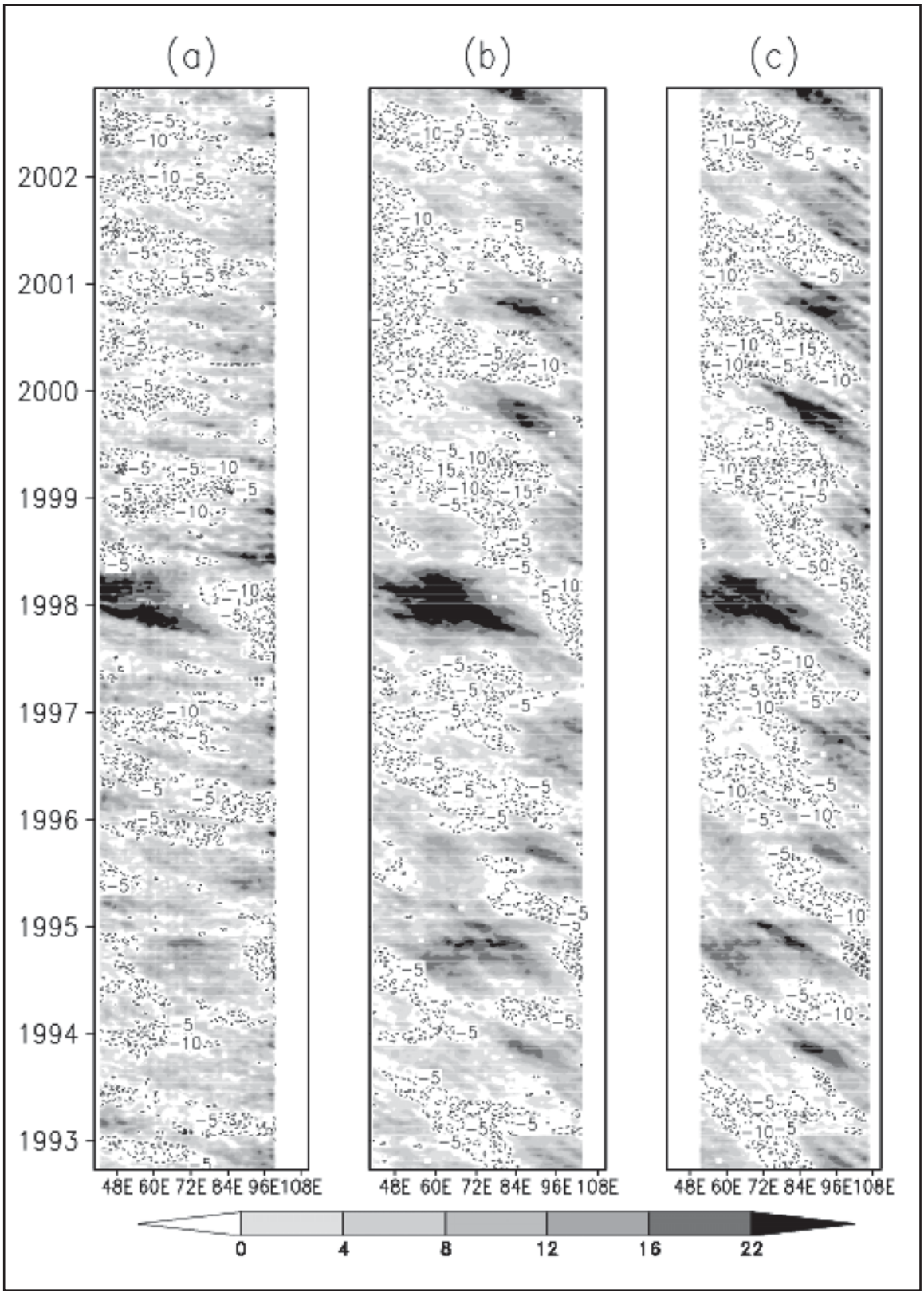

Figure 6. Longitude-Time plot of T/P SSHA (cm) (a) average of 5 .5°S to 2.5°S, (b) average 10.5°S and 5.5°S, (c) average 12.5°S and 7.5°S.

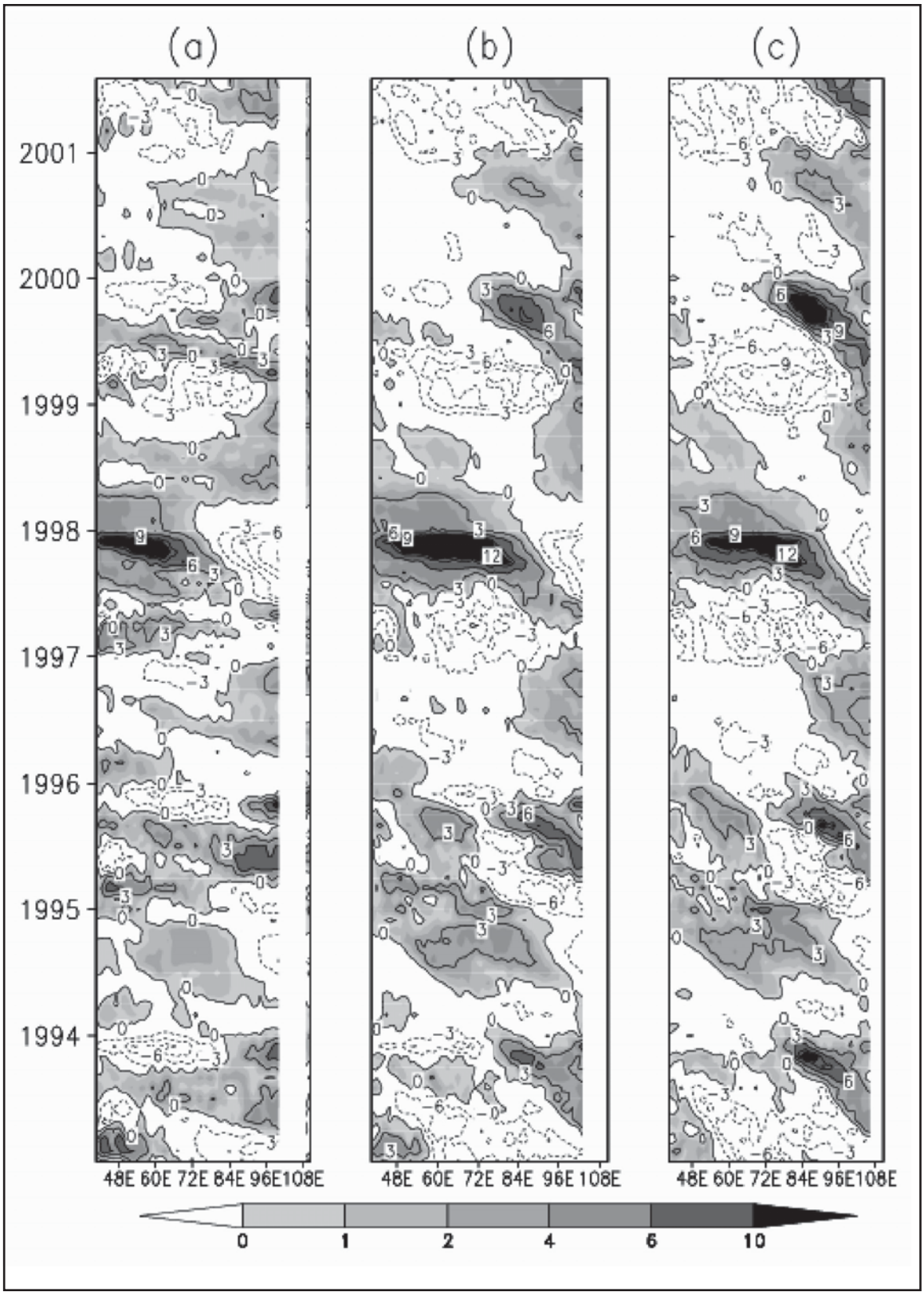

Figure 7. Longitude-Time plot of Heat storage anomalies (in 10^8 J/m^2) (a) average of 5 .5°S to 2.5°S, (b) average 10.5°S and 5.5°S, (c) average 12.5°S and 7.5°S.

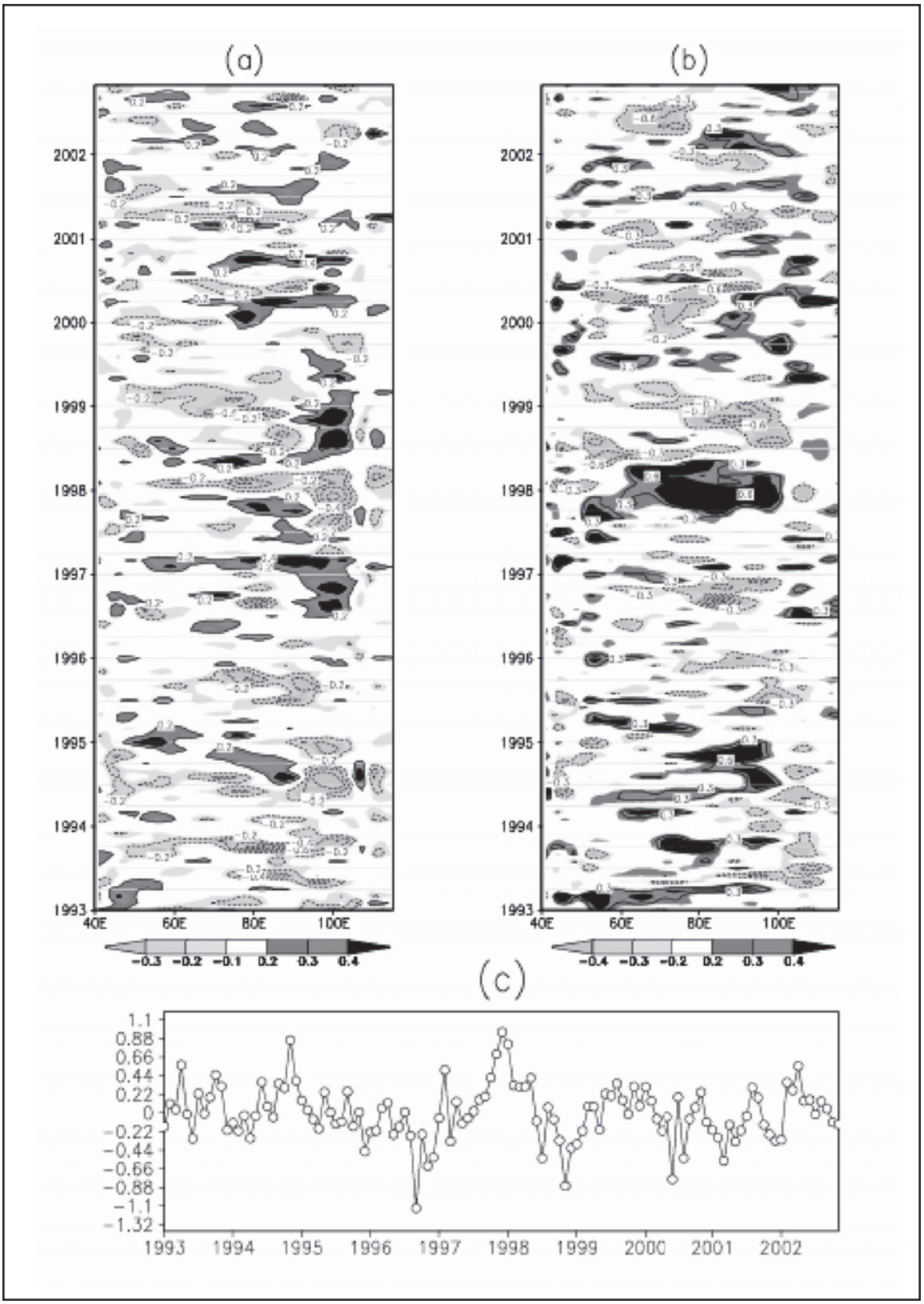

Figure 8. Longitude-Time plot of wind stress curl anomalies (*10^8dynes/cm^3) (a) average over 7°S –Equator, (b) Area average over 10°S - 7°S, (c) average over , 10°S - 7°S,80°-90°E.

al., 2002). The high SSHA and high HSA values in the central IO during October 1994 to February 1995 and October 1997 to February 1998 can be seen in Figs 6 and 7. This was also reported by Yu & Rienecker, (2000). Clear anomalous Rossby wave propagation in Fig. 6 and 7 especially in region south of 7°S during 1994-95 and 1997-98 (which has strengthened in 80-90°E) might have lead to warming in western IO. Figure 8 shows longitude-Time plot of wind stress curl anomalies (*10^8dynes/cm^3) (a) average over 7°S - Equator (b) average over 10°S - 7°S (c) area average over 10°S - 7°S, 80°-90°E. The anomalous propagation of Rossby waves (which strengthened in 80°-90°E) during 1994-1995 and 1997- 1998 might be the result of wind stress curl anomalies found in 80°-90°E during these periods. In other words these wind stresses curl anomalies are responsible (remotely) for early warming in 1998.Anomalous signals in 1997-1998 is found to be stronger than 1994 – 1995. This suggests that during dipole years the strong remote wind forcing has caused quick propagation of annual Rossby waves signals in the region south of 7.5°S. Thus Rossby wave's heat transporting property may be one of the reasons for maintaining high SST over the western IO in the early months of 1998.

A statistical study of T/P SSHA with special emphasis on IOD

The positive dipole mode events are associated with shallowing of the thermocline in the eastern IO and deepening in the western IO. During a negative dipole mode event the opposite pattern prevails. It has been found by Vinayachandran et al., (2002) that in the eastern IO the shallow thermocline corresponds to a thinner mixed layer and viceversa, but such a synchronous variation was not seen in the west. Statistical analysis has been done to study the positive and negative IOD mode. Figure 9 shows the correlations calculated in the eastern IOD box between the time series of parameters and a suitably fixed time (fixed based on peak IOD month which is given in Fig. 9) of the same parameter. Parameters chosen are HSA, biennial Rossby waves (resulted from FIR filters) and D20 anomalies. This gives a correlation series [say c(t)] for particular parameter. It is important here to note that the correlation series c(t) are spatial correlations of the cycle with a suitably fixed cycle. It was seen that positive and negative dipole years are inversely correlated. Moreover mean amplitude of c(t), which is given by $Ac = \sqrt{2}\,\sigma\,[c(t)]$ has also been calculated and given in Fig. 9. Significant differences have been observed in the Ac values during dipole and non-dipole years in heat storage anomalies, Rossby waves and in D20 anomalies. Now before applying similar procedure to western IOD box, we divided it into two regions, northern region say Region 1 [Equator - 10°N, 50° – 70°E,] and southern region say Region 2 [10°S- Equator, 50° – 70°E]. It was observed that both regions behave differently during different dipoles (Figure not shown). The Ac values calculated for Region 1 and Region 2 for different parameters are given in Table 1. The biennial Rossby waves in the northen box is very weak (Gnanaseelan et al., 2005) and so not considered in the analysis.

CEOF analysis of T/P SSHA and HSA

In order to study the interannual variability such as IOD, Complex Empirical Orthogonal Function (CEOF) analysis were carried out with T/P SSHA and HSA. The CEOF analysis captures both travelling as well as standing wave phenomenon in a single eigen function of a time series of a mapped anomalous data. Decomposition into CEOF allows to sort spatial structure that propagate in space and vary in time according to the decreasing variance (Barnett 1983). The real data series is transformed to the complex data series with the help of Hilbert transformation.

$$U(x,y,t) = u(x,y,t) + i\,\hat{u}\,(x,y,t)$$

where u is the original series and $\hat{u}$ has same amplitude as u but with the phase shift of 90°. The complex time series U can be decomposed into a set of orthogonal function in space $B_n(x,y)$ with the amplitude time function $A_n(t)$ and therefore

$$U(x,y,t) = \sum_n A_n(t)\, B_n(t)$$

The spatial amplitude function is given as

$$S_n(x,y) = [B_n(x,y)\, B_n^*(x,y)]^{1/2}$$

The spatial phase function is given as

$$Q_n(x) = \arctan \frac{\mathrm{Im}\, Bn(x)}{\mathrm{Re}\, Bn(x)}$$

Fig.10 shows the first and second CEOF modes of the SSHA and HSA. The first CEOF mode of T/P SSHA and HSA explains 30.13% and 43.12% respectively of the total variance. The second CEOF mode of T/P SSHA and HSA explains 21.66% and 22.48% respectively of the total sea-level variance in the TIO. The spatial pattern of the second mode clearly showed dipole structure. Infact both the first and second modes of the HSA had shown more % variance than SSHA. Moreover phase also showed westward propagation in the tropical IO. This is in

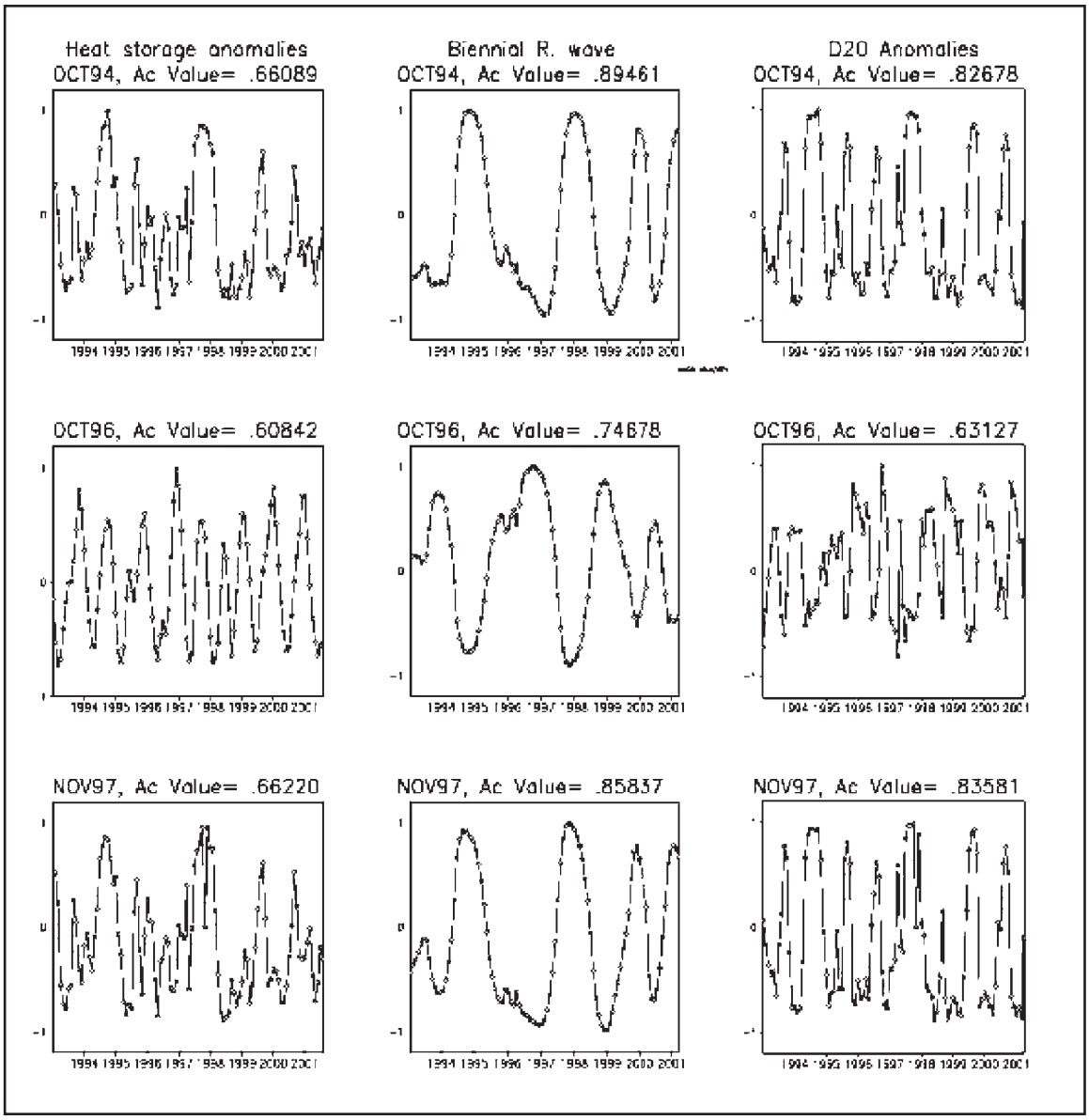

Figure 9. Correlation coefficient calculated in the Domain 10°S - Equator, 90°E -110°E.

agreement with the seesaw oscillation observed between the eastern and western equatorial IO thermocline depths identified previously by Masumoto & Meyers (1998), Basu, Meyers & O'Brien (2000) and Murtugudde & Busalacchi (1999). Moreover it is noticed that SSHA and HSA to the south of the equator in the western IO is elongated southeastward and its intensity is stronger than its northern counterpart (Fig.10b). It also reveals that the significant amount of interannual variability is confined to the north of 15°S. Using the extended EOF analysis of T/P SSHA, Rao et al., (2002) illustrated how thermocline oscillations in the western IO region take the form of Rossby waves propagating from the east. They referred second mode as a quasi-biennial mode. Therefore it can be concluded that IOD has been the leading mode of the interannual variability of the upper ocean HSA.

Fig.11 shows the cumulative percentage contributions of most significant modes to the total variance of T/P SSHA and HAS. In both T/P SSHA and HAS, the first three modes are found to explain maximum percentage of total variance. The rest of the modes occupied a very small percentage of total variance. Moreover number of modes to explain total variance in HSA is very less as compared to TP SSHA.

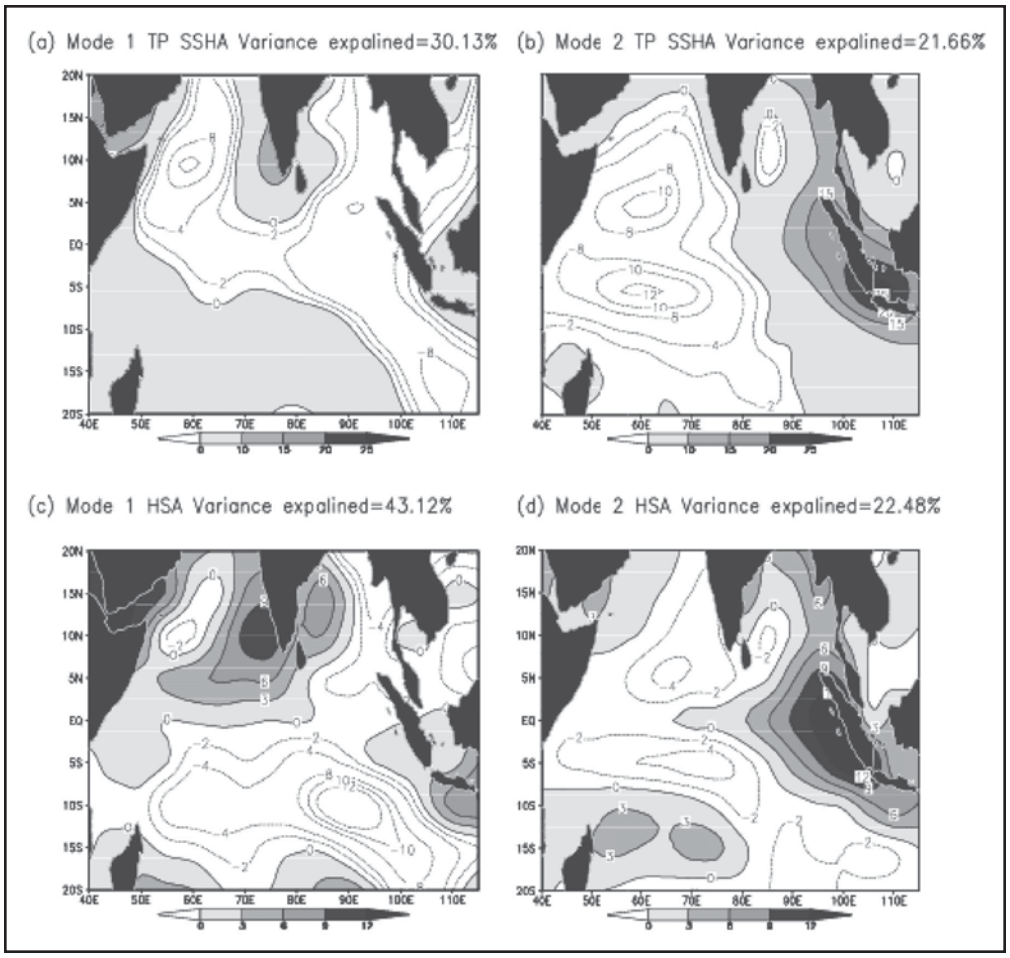

Figure 10. First and second CEOF modes of the T/P SSHA and HSA.

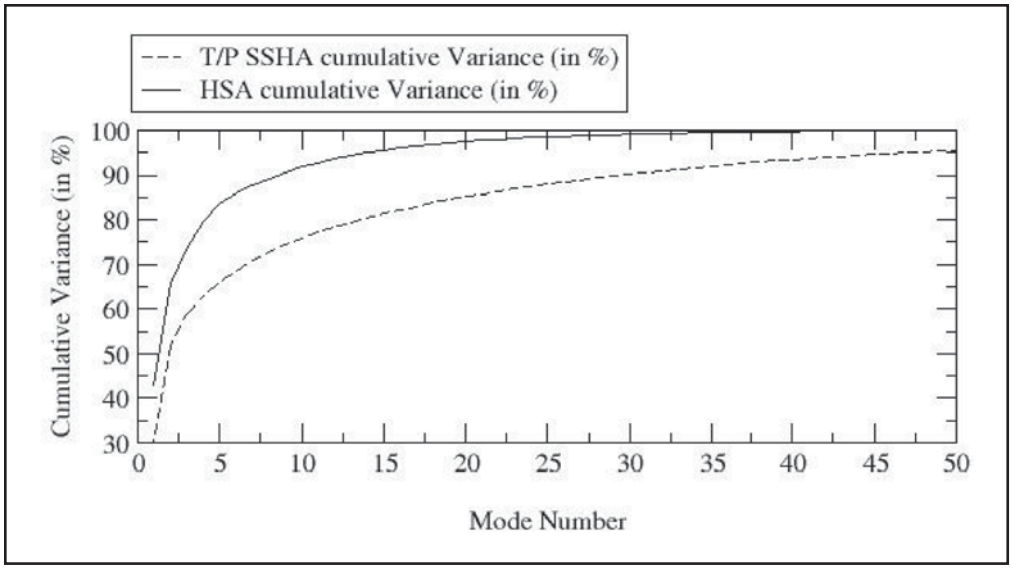

Figure 11. Cumulative variance (in %) of T/P SSHA and HSA.

This has strengthened the importance of HSA in studying the interannual variability such as IOD.

CONCLUSIONS

IOD has been shown to be a leading mode of the interannual variability of the upper ocean heat content and SSHA. Normally it has been found that the SST is low in the western IO and high in the eastern IO. But in some years this SST gradient reverses and causes shifting of convective activities over the western equatorial IO. This has been identified as IOD. A positive IOD is characterized by cool SST anomaly in the south eastern tropical IO and warm SST anomaly in the western tropical IO. Whereas a negative IOD is characterized by anomalously warm SST in the south eastern tropical IO and anomalously cold SST in the western tropical IO. T/P altimeter SSHA data has been found to be the strong effect of the ocean dynamics in the equatorial IO. The T/P measurement showed large SSHA in the western equatorial Indian Ocean during 1994-1995 and 1997 -1998 IOD events that represent the oceanic response to the surface wind forcing. These SSHA in turn played an important role in forming the SST anomalies. For instance, the equatorial surface warming in the western ocean was enhanced when the westward propagating positive SSHA arrived the western coast. The warm–west/ cold–east pattern that prevailed during IOD time was also accompanied by a large anomalous tilting of the thermocline. The relatively weaker 1994 warm event in the tropical IO also showed some similar features. Rossby waves play an important role in the interannual variability in the tropical IO, such as IOD and have been found to be influencing the IOD formation. In spite of their small surface signature, Rossby waves are clearly detected by SSHA and its filtered components. Further in 1994 peak cooling is seen in October (of the order of -4 x 10^8 J/m^2) and this cooling extend has been found to cover the longitudinal distance from 110°E to 85° E of IO. But in 1997 peak value of cooling is found in November 1997 (of the order of -15 x 10^8 J/m^2) and extend from 110°E to 68°E. Wind stress curl anomalies are playing an important role in strengthening Rossby waves in 80-90°E during the IOD years. Rossby waves are favorable for maintaining high SST over the western IO in the early months of 1998. It was seen that positive and negative dipole years are inversely correlated.

ACKNOWLEDGEMENTS

We thank Director, IITM for providing the infrastructure required for the study. We acknowledge Dr. P. S. Polito (Instituto Oceanográfico da Universidade de São Paulo (IOUSP), Brazil, for providing FIR filter and his critical suggestions have improved the work. The financial support was provided by Department of Ocean Development, Govt. of India through DOD - INDOMOD project. The authors are thankful to the T/P team and AVISO altimetrie, NCEP/NCAR and HADISST team for data. We acknowledge Dr. D. P. Chambers for providing monthly thermal expansion coefficient for the IO region and Mick Spillane for CEOF program.

REFERENCES

Annamalai, H., Potemra, J., Murtugudde, R. & McCreary, J. P., 2003. Indian Ocean Zonal Mode: Its decadal modulation and links to the Pacific, J. Clim., 18, 302-319.

Ashok, K., Guan, Z. & Yamagata, T., 2001. Impact of the Indian Ocean Dipole on the relationship between the Indian monsoon rainfall & ENSO, Geophys. Res. Lett., 28, 4499-4502.

Barnett, T. P., 1983. Interaction of the monsoon & Pacific trade wind system at interannual time scales, 1; The equatorial zone, Mon. Weather Rev., 111, 756-773.

Basu, S., Meyers, S.D. & O'Brien, J.J., 2000. Annual and interannual sea level variations in the Indian Ocean from Topex/Poseidon observations and ocean model simulations, Geo. phys. Res., l05, 975-994.

Behera, S.K., Krishnan, R. & Yamagata, T., 1999. Unusual ocean - atmosphere conditions in the tropical Indian Ocean during 1994, Geophys. Res. Lett., 26, 3001-3004.

Behera, S.K., Salvekar, P.S. & Yamagata, T., 2000. Simulation of interannual SST variability in the tropical Indian Ocean, J Clim., 13, 3487–3489.

Chambers, D.P. & Tapley, B.D., 1997. Long -period ocean heat storage rates & basin scale heat fluxes from Topex, J. Geophys. Res., 102, 10525-10533.

Chambers, D. P., Tapley, B. D., & Stewart, R. H., 1998. Measuring heat storage changes in the equatorial Pacific: A comparison between TOPEX altimetry & Tropical atmosphere-Ocean buoys, J. Geophys Res., 103, 18,591-18,598.

Clark, C.O., Webster, P.J. & Cole, J. E., 2003. Interdecadal variability of the relationship between the Indian Ocean Zonal Mode & East African coastal rainfall anomalies J. Clim., 16, 548-554.

Feng, M. & Meyers, G., 2003. Interannual variability in the tropical Indian Ocean: A two-year time scale of Indian Ocean Dipole Deep-Sea Res. II, 50, 2263-2284.

Gill, A.E. & Niiler, P.P., 1973. The theory of the seasonal variability in the ocean, Deep Sea Res., 20, 141–177.

Gill, A.E., 1982. Atmosphere Ocean Dynamics, Academic Press, San Diego, California, 622.

Gnanaseelan, C., Chowdary, J.S., Mishra, A.K. & Salvekar, P.S., 2003. Indian Ocean Dipole mode events in a simple mixed layer ocean model, Indian J. Mar. Sci., 32, 294-304.

Gnanaseelan, C., Vaid, B.H., Polito, S.P. & Salvekar, P.S., 2005. Interannual variability of Rossby waves in the Indian Ocean & its impact on Indian Ocean Dipole, reviewed to J. Geophys. Res., (JGR-Oceans).

Hsiung, J., Newell, R. E. & Houghtby, T., 1989. The annual cycle of oceanic heat storage & oceanic meridional heat transport, Q. J. R. Meteorological Soc., 115, 1-28.

Jacobs, G.A., 1994. Decade scale trans Pcific propagation warming effects of El-Nino anomaly, nature, 370, 360-363.

Killworth, P.D. & Blundell, J., 1999. The effects of bottom topography on the speed of long extratropical planetary waves, J. Phys. Oceanogr., 29, 2689–2710.

Lareef, Z., Rao, A.S. & Yamagata, T., 2003. Modulation of Sri Lankan Maha rainfall by the Indian Ocean Dipole, Geophys. Res. Lett., 30, 101029/2002GL 015639.

Lau, N.C. & Nath, M. J., 2003. Atmosphere–ocean variations in the Indo- Pacific sector during ENSO episodes. J. Clim., 16, 3–20.

Li, T., Wang, B., Chang, C. P. & Zhang, Y.S., 2003. A theory for the Indian Ocean dipole mode, J. Atmos. Sci., 56 - 76.

Masumoto, Y. & Meyers, G., 1998. Forced Rossby waves in the southern tropical Indian Ocean, J. Geophys. Res. 103, 27589-27602.

Moisan, J.R. & Niiler, P., 1997. The seasonal heat budget of the North Pacific: Net heat flux & heat storage rates (1950-1990), J. Phys. Oceanogr., 28, 401-421.

Murtugudde, R. & Busalacchi, A. J., 1999. Interannual variability of the dynamics & thermodynamics of the tropical Indian Ocean, J. Clim., 12, 2300–2326.

Murtugudde, R., McCreary, J.P. & Busalacchi, A.J., 2000. Oceanic processes associated with anomalous events in the Indian Ocean with relevance to 1997–1998, J. Geophys. Res., 105, 3295–3306.

Polito, P.S., Sato, O.T. & Liu, W. T., 2000. Characterization & validation of the heat storage variability from TOPEX/POSEIDON at four oceanographic sites, J. Geophys. Res., 105, 16911-16921.

Prasad, T.G. & McClean, J.L., 2004. Mechanisms for anomalous warming in the western Indian Ocean during dipole mode events, J. Geophys. Res., vol. 109, doi: 10.1029/2003JC001872.

Rao, A.S., Behera, S.K, Masumoto, Y., & Yamagata, T., 2002. Interannual variability in the subsurface tropical Indian Ocean, Deep-Sea Res. II, 49, 1549-1572.

Saji, N .H., Goswami, B.N., Vinayachandran, P. N. & Yamagata, T., 1999. A dipole mode in the tropical Indian Ocean', nature, 401, 360-363.

Saji, N.H. & Yamagata, T., 2002. A view of the tropical Indian Ocean climate system from the vantage point of Dipole Mode events, J. Clim., 2500-2518.

Saji, N.H. & Yamagata, T., 2003. Possible Impacts of Indian Ocean Dipole Mode events on Global Climate, Clim. Res., 25, 151-169.

Samelson, R.M., 1992. Surface-intensified Rossby waves over rough topography, J. Mar. Res., 50, 367–384.

Vinayachandran, P.N., Iizuka, S., & Yamagata T., 2002. Indian Ocean Dipole mode events in an ocean general circulation model, Deep-Sea Res., II, 49, 1573-1596.

Vinayachandran, P. N., Saji, N. H. & Yamagata, T., 1999. Response of the equatorial Indian Ocean to an unusual wind event during 1994, Geophys. Res. Lett., 26, 1613-1616.

Wang, B., Wu, R. & Li, T., 2003. Atmosphere-warm ocean interaction & its impact on Asian-Australian monsoon variability J. Clim., 16, 1195-1211.

Webster, P.J., Moore, A.M., Loschnigg, J.P. & Leben, R. R., 1999. Coupled Ocean-Atmosphere dynamics in the Indian Ocean during 1997-98, nature, 401, 357-360.

White, B. W. & Tai, C. K., 1995. Inferring interannual changes in global upper ocean heat storage from TOPEX altimetry, J. Geophys. Res., 100, 24 943- 24, 954,

White, W. B., 1985. The resonant of inte-rannual barocilinic rossby waves to wind forcing in the eastern midlatitude North Pacific, J. Phys. Oceanogr., 15404-15415.

Wyrtki, K. & Uhrich, L., 1982. On the Accuracy of Heat Storage Computations, J. Phys. Oceanogr., 12, 1412-1416.

Xie, S. P., Annamalai, H., F. Schott, A. & McCreary, J. P., 2002. Structure & mechanisms of South Indian Ocean climate variability, J. Clim., 15, 864–878.

Yamagata, T., Behera, S.K., Rao, S.A., Guan, Z., Ashok, K. & Saji, N. H., 2002. The Indian Ocean Dipole: a Physical Entity, CLIVAR Exchanges, 7, 15-18.

Yan, X.H., Niiler, P.P. Nadaga ,S. K., Stewart, R. H., & Cayan, D. R., 1995. Seasonal Heat Storage in the North Pacificÿ1976-1989, J. Geophys. Res., 100, 6899-6926.

Yu, L. & Rienecker, M., 2000. Indian Ocean warming of 1997– 1998, J. Geophys. Res., 105, 16923–16939.

(Accepted 2005 August 23. Received 2005 May 6; in original form 2005 February 11)

Mr. B. H. Vaid presently working as Research Fellow in the Indian Institute of Tropical Meteorology, Pune. After graduating from Govt. Degree College Kathua (J&K), he did his Master in Physics from H. N. B. Garhwal, University, Garhwal. He felt a strong need to have clarity in thought, expression, hence he has also done B.Ed (Bachelor of Education) from Jammu University, Jammu. Further the field of Physics learned him as they were more chaotic in nature. Hence, he had done his second master's degree (M.Tech.) in Atmospheric physics, University of Pune, Pune. He is currently pursuing his Ph. D in Atmospheric Physics from Pune University, Pune, under the guidance of Dr. C. Gnanaseelan. He has participated in one International and many national conferences and presented research papers.

Dr. C. Gnanaseelan is a holder of an M.Sc. (Mathematics, 1989, Madurai Kamaraj University), M.tech (Atmospheric Science & Technology, 1991, IIT Kharagpur) and Ph.D. (Mathematics, 1998, IIT Kharagpur). From Nov. 1993 to Jan. 1999, he was a Research Assistant in CWPRS, Pune and subsequently joined as a Scientist in the Indian Institute of Tropical Meteorology, Pune. Presently he is working as Scientist - C in the same Institute. He has to his credit 16 scientific papers in renowned International and National journals and also contributed 7 papers published in proceeding/books. The university of Pune bestowed him with the title 'Adjunct Professor', Department of Physics, University of Pune, Pune, India.

Mr. Bijoy Thompson presently working as Senior Research Fellow, in the Indian Institute of Tropical Meteorology, Pune. After graduating from University of Kerala, he went on to do his Master in Meteorology from Cochin University of Science and technology. He is currently pursuing his Ph. D in Atmospheric Physics from Pune University, Pune, under the guidance of Dr. C. Gnanaseelan. He has participated in one International and many National conferences and presented research papers.

Ms. Ayantika De presently working as research fellow in the Indian Institute of Tropical Meteorology, Pune. After graduating from BHU, she went on to do her Master in Physics and there by after M. Tech. in Atmospheric Physics from Pune University. She is currently pursuing her Ph. D in Atmospheric Physics from Pune University, Pune, under the guidance of Dr. R. Krishnan. She has participated in one National conference and presented research paper.

Dr. (Mrs.) P. S. Salvekar has obtained post graduate in Applied Mathematics, and Ph.D. in Atmospheric Physics from Pune University, Pune. She has 30 years Research experiences in Meteorology. Presently, she is working as Scientist –F, Head of Theoretical Studies Division, Indian Institute of Tropical Meteorology, Pune. She has to her credit 86 scientific papers in renowned International and National journals. She has been recipient of two awards: WMO young Scientist Award (International) and Mausam Award (National). She has been also working as visiting Prof. in Pune University since last 20 years. She has examined many Ph. D thesis form Pune University and IITs. Under her guidance six students have been awarded Ph.D. She is specialized in Monsoon Dynamics, Instability studies, Atmospheric Energetics and Modelling in Atmospheric and Oceanic Circulation.